CHAPTER IV
RESULTS AND DISCUSSION

4.1 Preparation of Sericin

4.1.1 FT-IR Characterization

Sericin [Fig. 4.1(g)] showed absorption bands at 3315 cm^{-1} (NH stretching), 1650 cm^{-1} (amide I, CO stretching), 1540 cm^{-1} (amide II, NH bending), 1237 cm^{-1} (amide III, CN stretching), and 669 cm^{-1} (amide V). These results corresponded to IR spectrum of sericin in previous works (Sarovart, *et al.* 2003; Cho, *et al.* 2003, Teramoto, *et al.* 2004) and confirmed that we have successfully prepared sericin from silk cocoon.

4.1.2 ^{1}H-NMR Characterization

The chemical shifts of sericin (Table 4.1) showed significant peaks of rich amino acid. The β-CH_2 and α-CH resonance of the serine appeared at 3.633 and 4.093 ppm, respectively. The aromatic protons of the tyrosine appeared as doublet peaks at 6.553 and 6.828 ppm (Gotoh, *et al.*1993; Cho, *et al.* 2003).

Table 4.1 ^{1}H-NMR chemical shifts of sericin

Material	Chemical shift (ppm)	Type of proton	Chemical structure
Sericin	3.633	Ser β	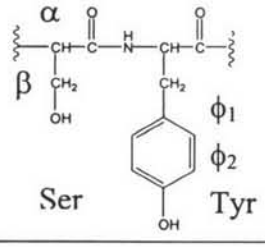
	4.093	Ser α	
	6.553	Tyr ϕ_1	
	6.828	Tyr ϕ_2	

4.1.3 Thermal Gravimetry Characterization

The TG/DTA results of sericin (Table 4.3) showed two steps of weight loss. At 66°C absorbed moisture was lost in the sample and decomposition temperature was presented at 306°C, with 65% of weight loss values.

4.2 Modified Sericin by Solution Blending (SS/PAM)

4.2.1 FT-IR Characterization

The IR spectrum of PAM [Fig. 4.1(a)] showed strong bands at 3400 and 3200 cm^{-1} that was amide N-H stretching. Two strong bands at 1655 and 1600 cm^{-1} were C=O stretching and N-H bending. The vibration modes of primary amide group showed at 620 cm^{-1}.

The IR spectra of the 10/90, 20/80, 30/70, 40/60, and 50/50 of SS/PAM blend film [Fig. 4.1(b)-(f)] were characterized by the presence of the absorption bands of the pure components such as the amide II and amide III of sericin, and N-H bending of PAM. The same results of previous study, (Freddi, *et al.* 1999) also reported that molecular interactions mainly based on hydrogen bonding were established between silk fibroin and PAM chains.

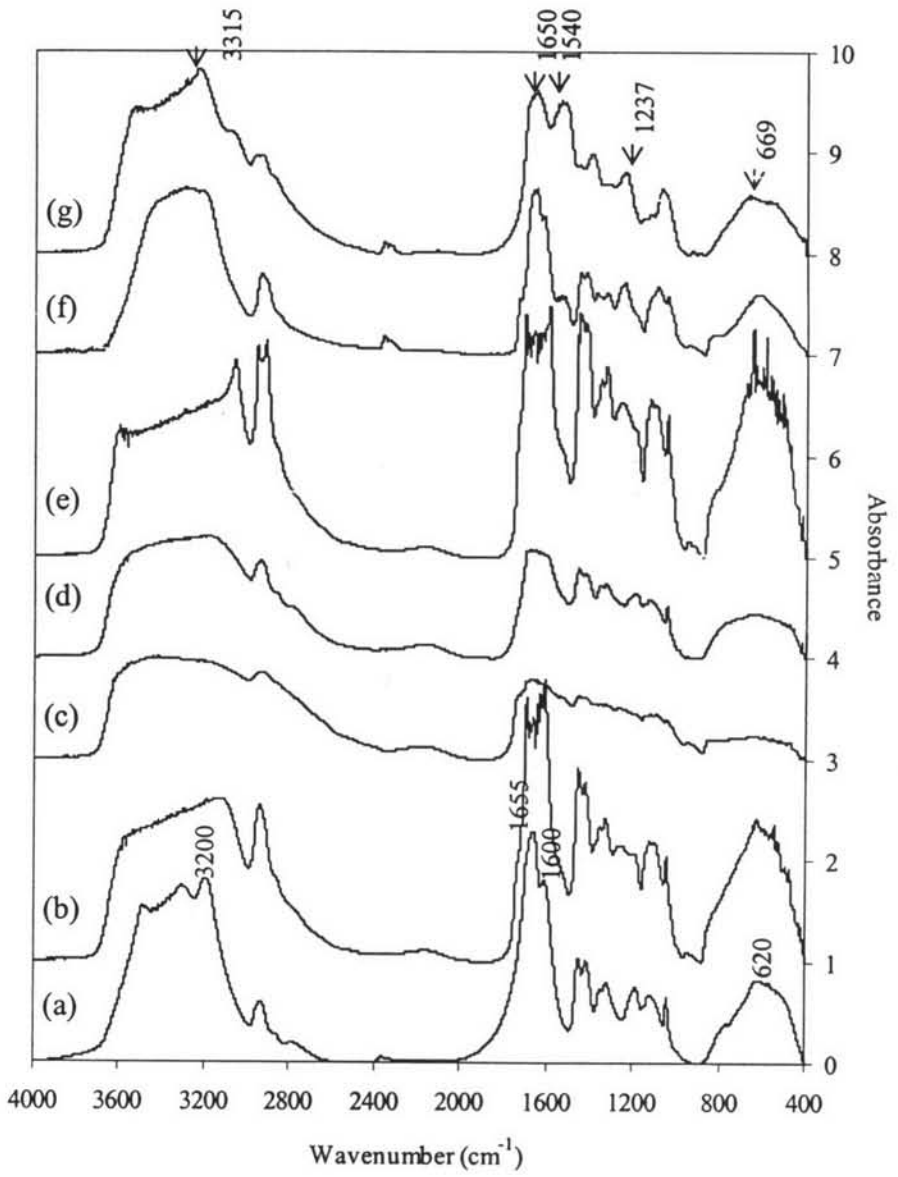

Figure 4.1 IR spectra of modified sericin by solution blending (SS/PAM): PAM (0/100) (a), 10/90 (b), 20/80 (c), 30/70 (d), 40/60 (e), 50/50 (f), and sericin (100/0) (g).

4.2.2 ^{1}H-NMR Characterization

The ^{1}H-NMR spectra of the 10/90, 20/80, 30/70, 40/60, and 50/50 of SS/PAM blend (Table 4.2) were characterized by the presence of the chemical shift of proton in sericin such as Ser β and polyacrylamide. From the result of both FTIR and ^{1}H-NMR, we concluded that the molecular interactions mainly based on hydrogen bonding, were established between sericin and PAM chains (see Fig. 4.2).

Table 4.2 ^{1}H-NMR chemical shifts of modified sericin by solution blending (SS/PAM)

SS/PAM (w/w)	Chemical shift (ppm)			
	Proton of sericin	Proton of PAM		
	Ser β	H^{β}	H^{α}	H^{γ}
0/100	-	1.425	1.978	6.781
10/90	3.633	1.505	2.042	6.761
20/80	3.602	1.504	2.041	6.770
30/70	3.656	1.505	2.059	6.795
40/60	3.661	1.503	2.058	6.780
50/50	3.655	1.501	2.040	6.791
100/0	3.633	-	-	-

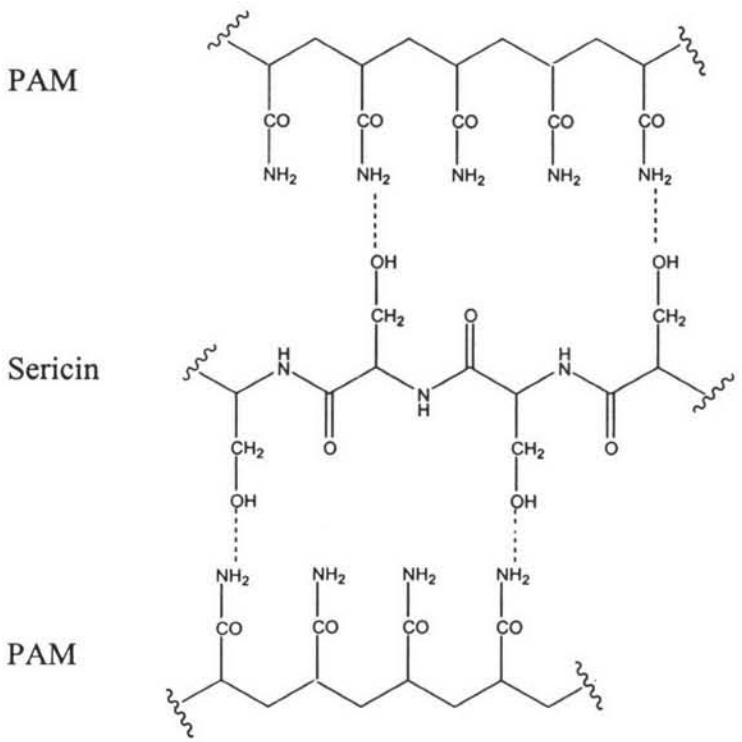

Figure 4.2 Molecular interactions between sericin and PAM chains.

4.2.3 Thermal Gravimetry Characterization

The TG/DTA results of PAM, and SS/PAM blend in nitrogen atmosphere are shown in Table 4.3. In the case of PAM, three distinct zones were observed where the weight was being lost. The initial weight loss at 70°C was due to the presence of small amount of moisture in the sample. The second loss was due to the loss of NH_2 group in the formation of ammonia, with 18% of weight loss values at 295°C. In this temperature range, the formation of imide groups via cyclization could occur and the decomposition of cyclized imide groups were observed 40% of weight loss values at 340°C. This result also reported in Biswal, *et al.* 2004. From TG/DTA curves of SS/PAM blends found four steps of weight loss. The first step was due to the loss of water in sample. In step 2 and 3 were the decomposition of PAM. The last step showed weight loss of high molecular weight species that due to the condensation between amine groups of PAM and hydroxyl groups of sericin. This result demonstrated that the intermolecular of SS/PAM blend greatly improved the thermal stability of materials. The degradation temperature and %weight loss of SS/PAM blend in different ratios showed in Table 4.3. The degradation temperature of high molecular weight species decreased when sericin content increased. Wang, *et al.* (1997) described the poly(acrylonitrile-acrylamide-acrylic acid)[P(AN-AM-AA)]/poly(vinyl alcohol)(PVA) intermacromolecular complex formed through hydrogen bonding. From thermal decomposition results, they found that the P(AN-AM-AA)/PVA complex had 60°C higher than that of P(AN-AM-AA).

Table 4.3 Temperature degradation and % weight loss of modified sericin by solution blending (SS/PAM)

SS/PAM (w/w)	Step of weight loss								% Char
	Water		NH_2 groups		Imide groups		High MW species		
	Td_1 (°C)	%wt loss	Td_2 (°C)	%wt loss	Td_3 (°C)	%wt loss	Td_4 (°C)	%wt loss	
0/100	70	12.2	294	17.5	343	39.5	-	-	30.8
10/90	<200	9.3	289	17.7	345	30.6	564	39.5	2.9
20/80	<200	11.0	283	15.4	352	27.4	528	40.0	6.2
30/70	<200	15.8	278	14.3	346	27.1	521	34.3	8.5
40/60	<200	17.5	281	11.0	345	31.7	522	37.2	2.6
50/50	<200	10.5	278	17.5	345	24.5	515	43.7	3.8
100/0	70	8.0	Decomposition of sericin: 306°C, 65.0%						27.0

4.3 Electrospinning of Modified Sericin (SS/PAM)

4.3.1 Scanning Electron Microscope Characterization

In the case of PAM, it was successfully electrospun at 40 %wt and 50 % wt with 25 kV of applied high voltage. Fig. A24 showed nanoparticles of 40 %wt PAM. Most of them were free spherical beads and some were connected by nanofibers of diameter 102 nm. On the other hand, the 50 %wt of PAM was spun into nanofibers, and the size ranged at 185 nm as average diameter. These results led to the electrospinning of modified sericin through blending and chemical reaction.

SEM images of modified sericin by solution blending were shown in Fig. 4.3-4.9. The morphology of sericin electrospun at 25 kV with magnification of 1000 was particles like a flake. Due to sericin consisting of serine and aspartic acid

were major components, respectively. The esterification reaction can be occurred when one component is higher than another one. This results in crosslinking and gel formation. Therefore, it was hardly spin sericin into nanofibers. In the case of PAM, it was successfully electrospun between 15 and 25 kV (Fig. 4.3). The morphology of PAM with magnification of 5000 was continuous fibrous structure. The average diameter of size was 185 nm. When the amount of sericin was 10 %wt, the morphology of electrospun product showed continuous fibers and the best condition for electrospun nanofibers was using 20 kV of applied high voltage which gave nanofibers having average of diameter 129 nm smaller than that of pure PAM electrospun fibers. Increasing the sericin content up to 50 %wt, the morphology by electrospinning showed aggregates particles and bulky structure. This result suggested that the intermolecular bonding between sericin and PAM to form gel can be minimized and hence cannot interfere much on electrospinning process.

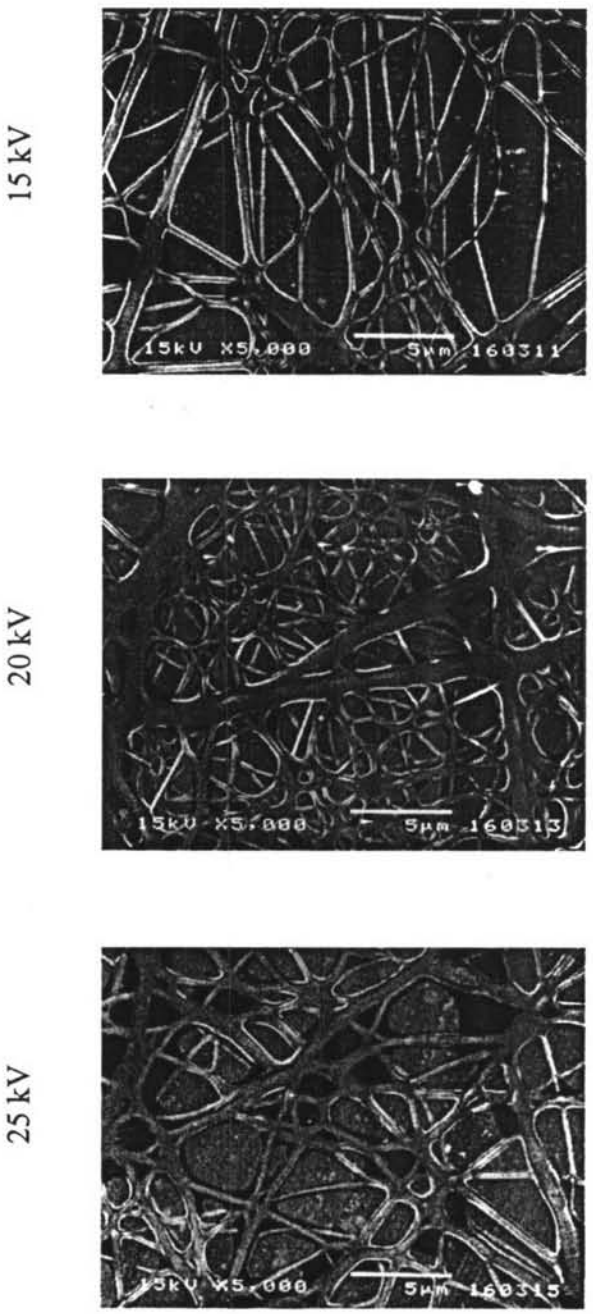

Figure 4.3 SEM images (at magnification of 5000 and scale bar shown is for 5 µm) of electrospun of PAM 50 %wt in water.

Figure 4.4 SEM images (at magnification of 5000 and scale bar shown is for 5 μm) of electrospun modified sericin (SS/PAM) by solution blending in water: 10/90 w/w of SS/PAM.

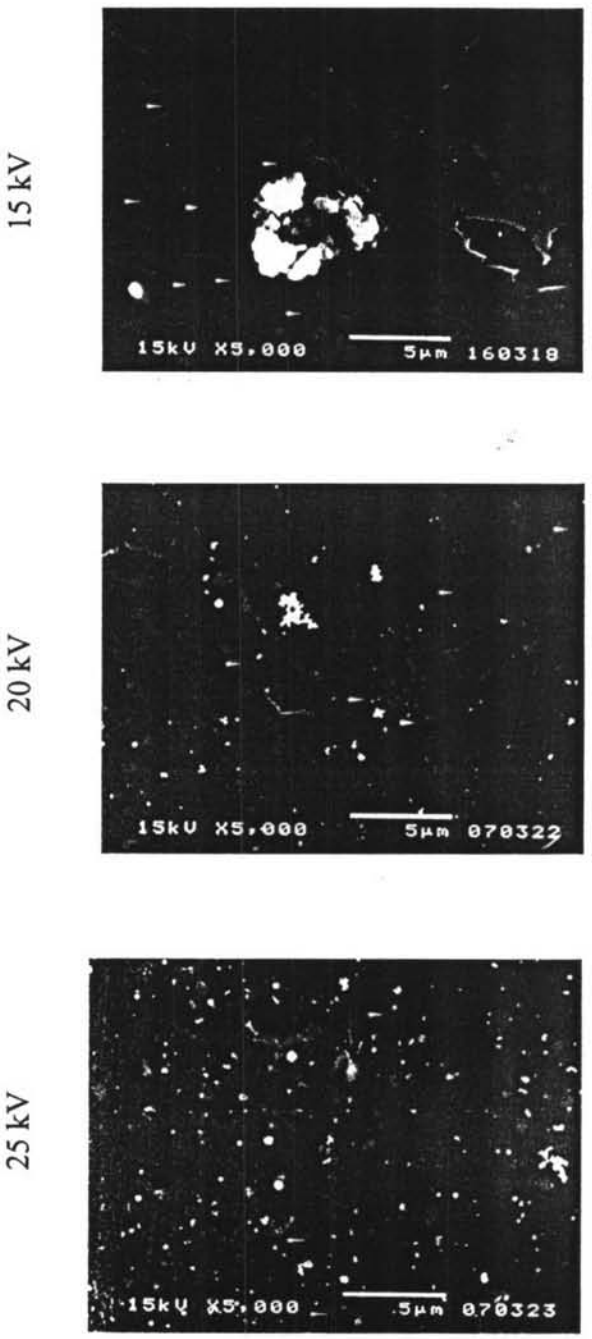

Figure 4.5 SEM images (at magnification of 5000 and scale bar shown is for 5 µm) of electrospun modified sericin (SS/PAM) by solution blending in water: 20/80 w/w of SS/PAM.

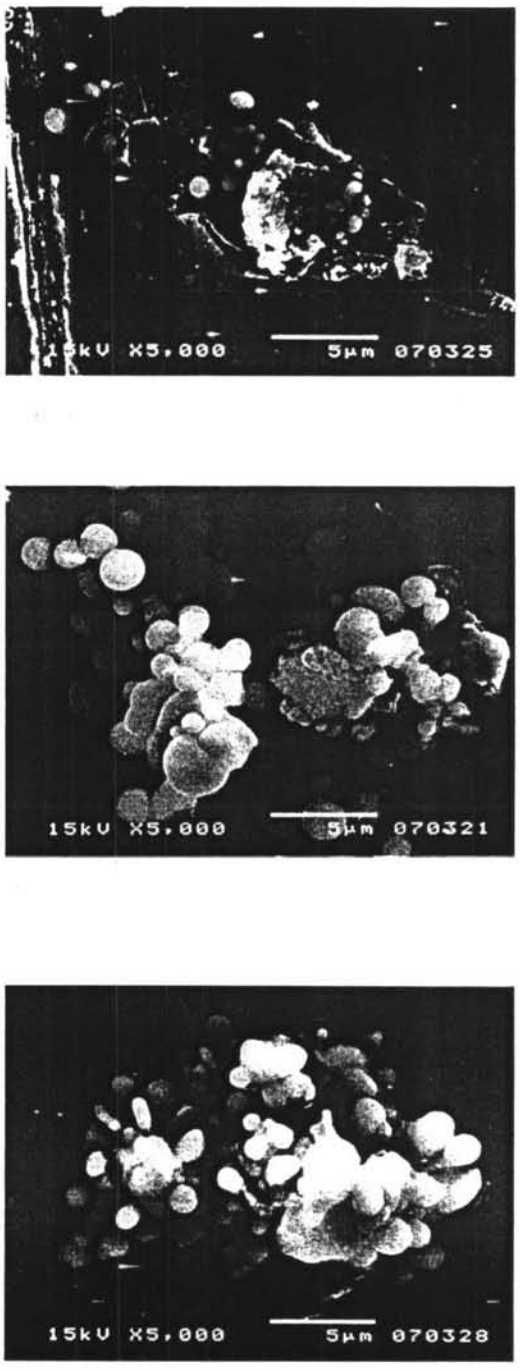

Figure 4.6 SEM images (at magnification of 5000 and scale bar shown is for 5 µm) of electrospun modified sericin (SS/PAM) by solution blending in water: 30/70 w/w of SS/PAM.

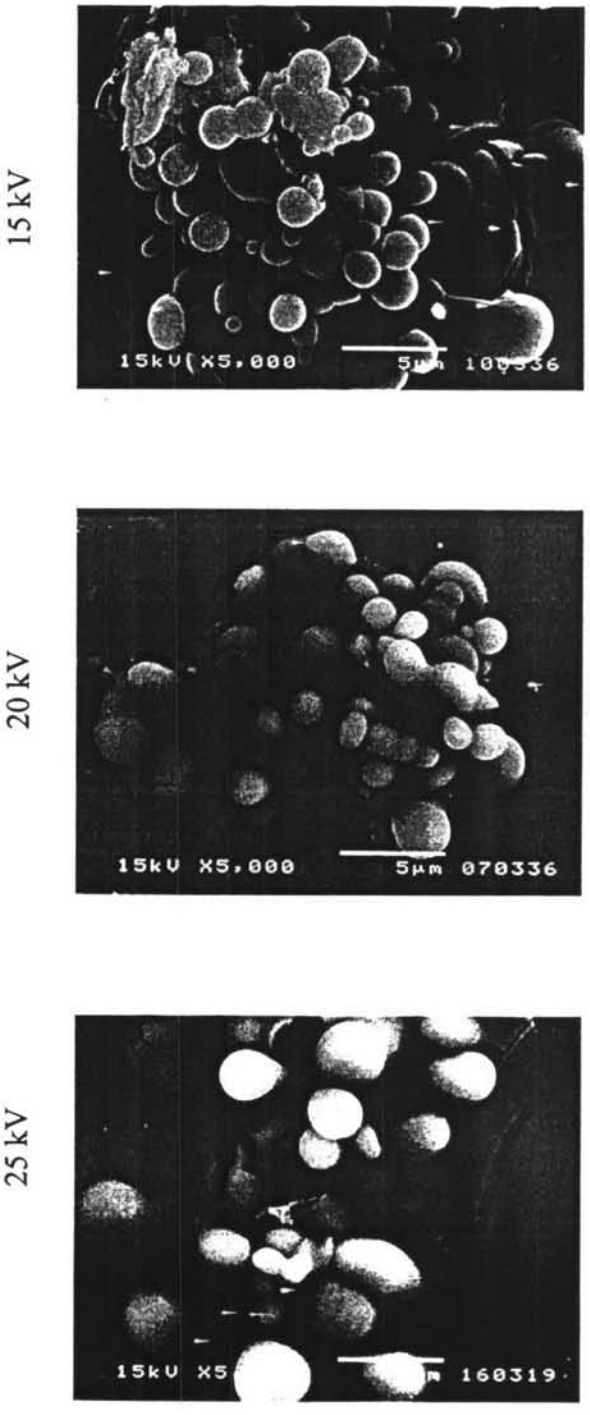

Figure 4.7 SEM images (at magnification of 5000 and scale bar shown is for 5 µm) of electrospun modified sericin (SS/PAM) by solution blending in water: 40/60 w/w of SS/PAM.

Figure 4.8 SEM images (at magnification of 5000 and scale bar shown is for 5 µm) of electrospun modified sericin (SS/PAM) by solution blending in water: 50/50 w/w of SS/PAM.

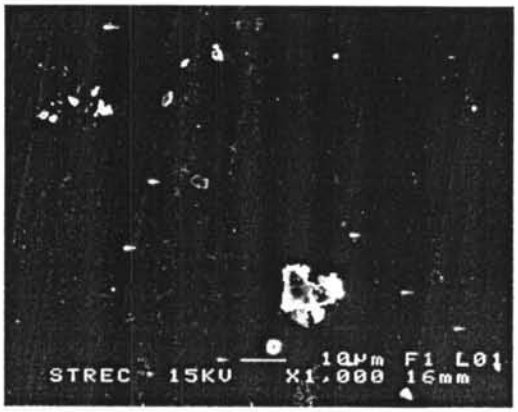

Figure 4.9 SEM image (at magnification of 1000 and scale bar shown is for 10 µm) of electrospun sericin 10 %wt in water at 20 kV.

4.4 Modified Sericin by Chemical Reaction (SS-PAM)

4.4.1 Preparation of PAM Derivative **a**

The amide groups of PAM were less reactive than primary amine due to lone pair electron of nitrogen were attracted by carbonyl group. This result led to change these groups to primary amine by reacting with ethylenediamine (Fig. 4.10).

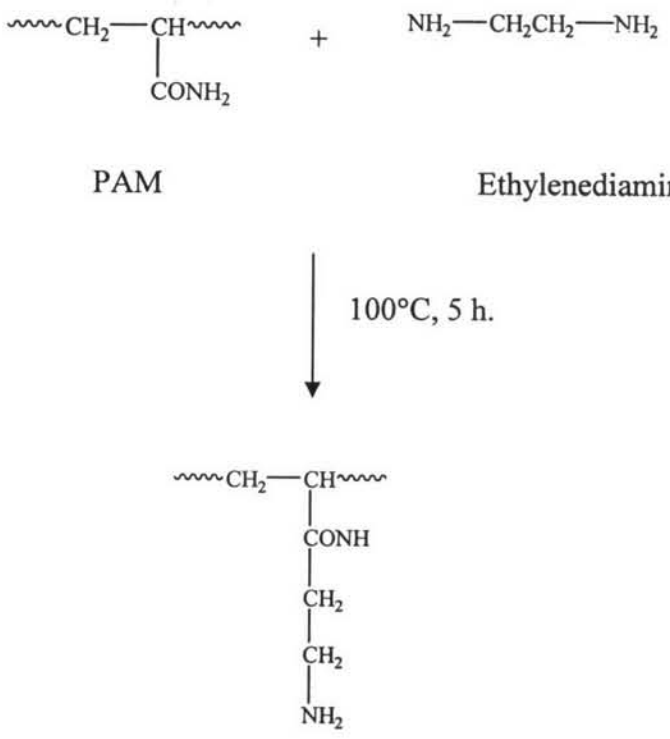

Figure 4.10 Chemical reaction of PAM derivative **a**.

4.4.1.1 FT-IR Characterization

From IR spectrum of PAM derivative **a** [Fig. 4.11(b)] was similarly to IR spectrum of PAM. In contrast, it showed broad band from 3200 to 3400 cm^{-1} that belonged to N-H stretching of mono substitute amide.

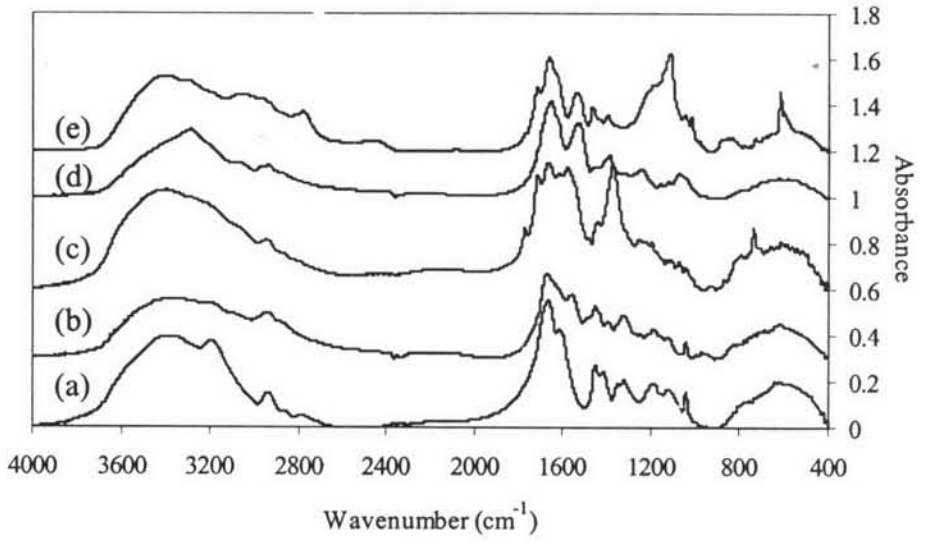

Figure 4.11 IR spectra of PAM (a), PAM derivative **a** (b), PAM derivative **b** (c), Sericin (d), and modified sericin by chemical reaction (SS-PAM) (1:1 w/w) (e).

4.4.1.2 ^{1}H-NMR Characterization

The chemical shift of PAM derivative **a** was shown in Table 4.4. Four environments of proton were observed in chemical shift 1.382, 1.922, 2.647, and 3.037 ppm, respectively.

Table 4.4 ^{1}H-NMR chemical shift of PAM derivative **a**

Chemical shift (ppm)	Type of proton	Chemical structure
1.382	H^a	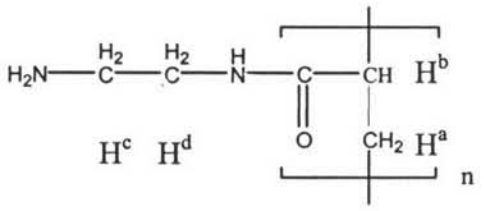
1.922	H^b	
2.647	H^c	
3.037	H^d	

4.4.1.3 Thermal Gravimetry Characterization

In PAM derivative **a** showed three steps of weight loss (Fig. 4.12). The first step showed weight loss of small amount of solvent including water and ethanol at 78°C. The second step was due to the loss of ethylenediamine (bp = 118°C), with 18% of weight loss values at 209°C. The last step, the degradation temperature of PAM derivative **a** was observed with 59.8% of weight loss at 350°C.

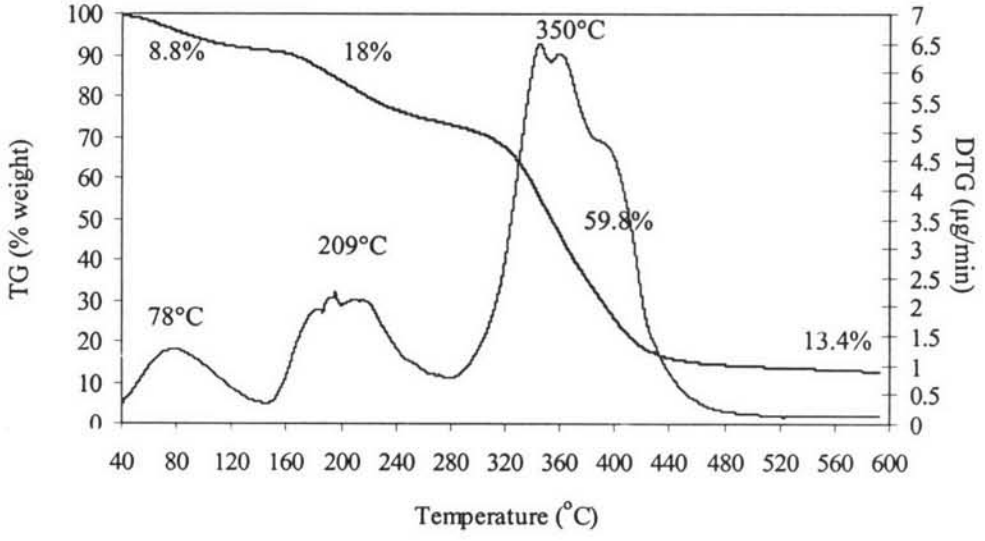

Figure 4.12 TG/DTA curves of PAM derivative **a**.

4.4.2 Preparation of PAM Derivative **b**

The reactive amine groups of PAM derivative **a** reacted with trimellitic anhydride in DMF (Fig. 4.13). However, the side group of trimellitic anhydride consists of anhydride and carboxylic groups, the anhydride group is more reactive than another one. Under high temperature conditions, the reaction leads to open ring of anhydride with reactive amine groups and form imide group (-CO-NH-CO-) via cyclization.

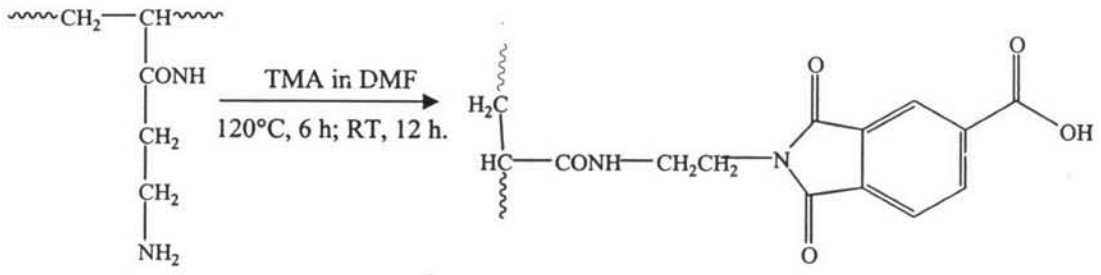

PAM derivative **a** PAM derivative **b**

Figure 4.13 Chemical reaction of PAM derivative **b**.

4.4.2.1 FT-IR Characterization

The IR spectrum of PAM derivative **b** [Fig. 4.11(c)] showed broad band about 3400 cm^{-1} corresponding to carboxylic acid O-H and amide N-H stretchings, strong bands at 1710 and 1650 cm^{-1} corresponding to C=O stretching of carboxylic acid and amide group, respectively. The band around 1777 was for symmetric C=O of imide group. Moreover, at 1371 and 731 cm^{-1} showed C-N stretching and C=O bending of imide group, respectively.

4.4.2.2 ^{1}H-NMR Characterization

The chemical shift of PAM derivative **b** was shown in Table 4.5. The chemical shift of H^{c} and H^{d} shifted to downfield. This shift was the result of the shielding effects of imide group on the structure. Moreover, the protons of benzene ring were observed around 7 to 8 ppm.

Table 4.5 ^{1}H-NMR chemical shift of PAM derivative **b**

Chemical shift (ppm)	Type of proton	Chemical structure
1.220	H^a	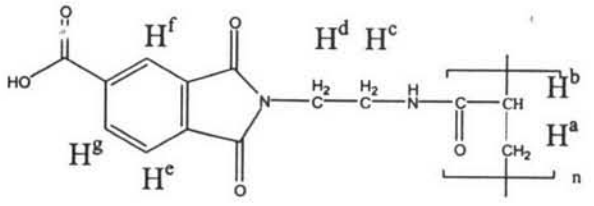
2.309	H^b	
2.711	H^c	
2.871	H^d	
6.928	H^e	
7.077	H^f	
7.933	H^g	

4.4.2.3 Thermal Gravimetry Characterization

The four steps of weight loss were observed in PAM derivative **b** (Fig. 4.14). The initial and second of weight loss came from ethanol and DMF at 65 and 158°C, respectively. The degradation temperature at 257°C belonged to trimellitic anhydride (TMA) residues about 14% of weight loss (Td of TMA = 250°C). The last step was due to the loss of imide group, with 36.6% of weight loss values at 394°C. These results concluded that the PAM derivative **b** showed higher thermal resistance of imide groups and had more thermal resistance than PAM derivative **a**.

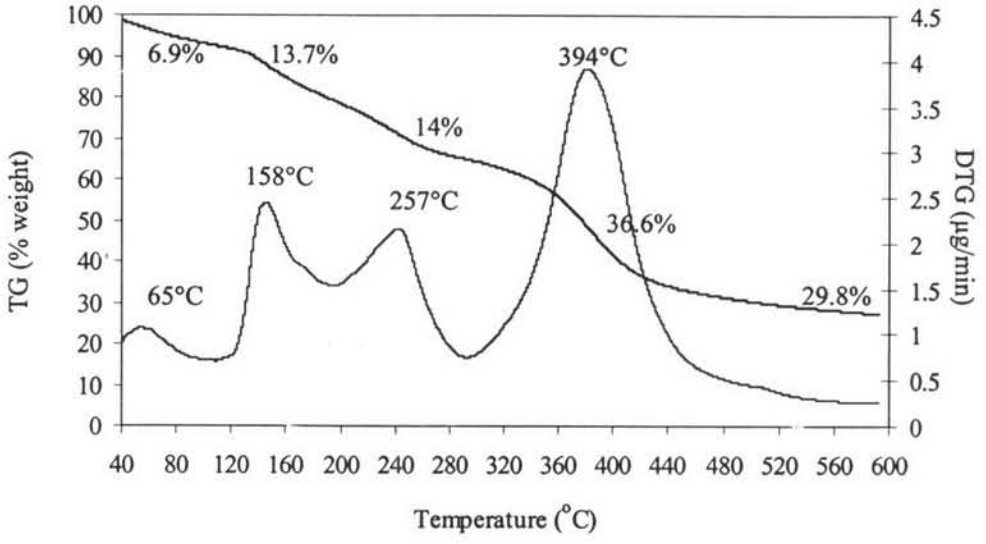

Figure 4.14 TG/DTA curves of PAM derivative **b**.

4.4.3 Preparation of Modified Sericin (SS-PAM)

Modified sericin (SS-PAM) was obtained by esterification reaction between the reaction site of sericin and PAM derivative **b** under acid condition (Fig. 4.15). The hydroxyl group (i.e. serine, tyrosine) in sericin reacted with the protonated PAM derivative **b** in carboxylic acid. All of these results were indicated by the FTIR, ^{1}H-NMR, and thermal gravimetry characterization.

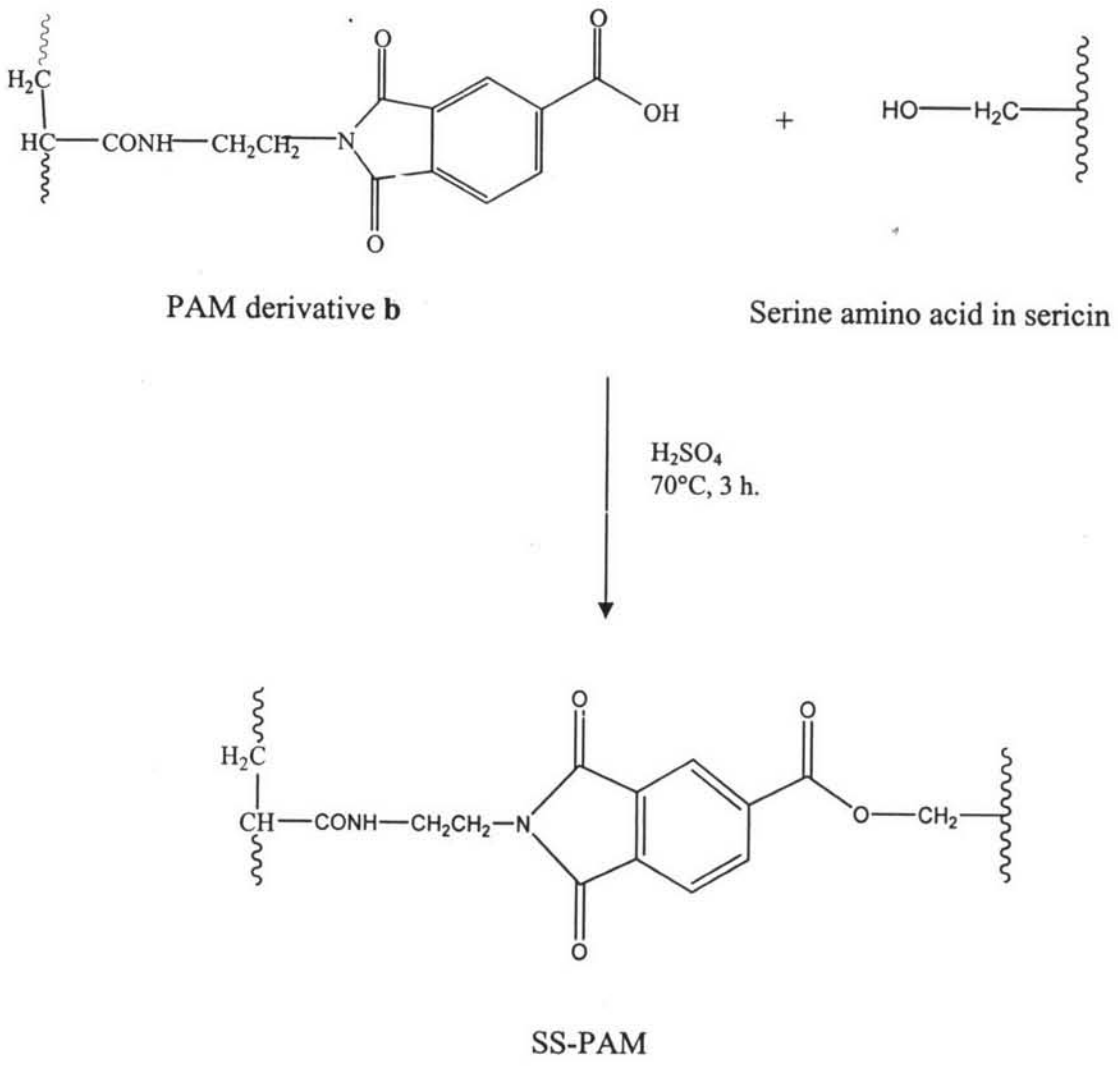

Figure 4.15 Chemical reaction of modified sericin (SS-PAM).

4.4.3.1 FT-IR Characterization

IR spectrum of SS-PAM modification was shown in [Fig. 4.11(e)]. The new peaks were found in SS–PAM modification including N-H bending of sericin (amide II) at 1540 cm^{-1}, C=O stretching of aromatic ester and C-O stretching of ester at 1720 and 1197 cm^{-1}, respectively. Moreover, the board peak of O-H stretching of carboxylic acid was disappeared.

These results indicated that the carboxylic acid groups of PAM derivative **b** were reacted by the hydroxyl group of sericin in acid condition.

FT-IR spectra of modified sericin (SS-PAM) in different ratios were shown in Fig. 4.16. The absorption band at 1720 cm^{-1} was C=O stretching of aromatic ester. The band at 1197 and 1110 cm^{-1} belonged to C-O stretching of ester in asymmetric trisubstitute benzene because the hydroxyl group could be reacted at the imide sites. The hydroxyl group preferred to react with protronated carboxylic acid sites than another one because this group had highly lack of electrons and less steric hindrance site.

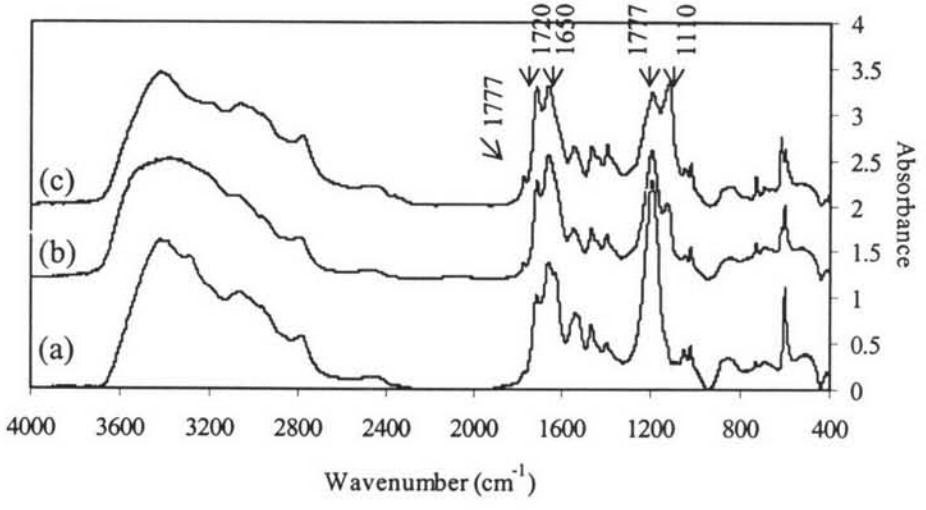

Figure 4.16 IR spectra of SS-PAM modification 1:1 (a), 1:5 (b), 1:10 (c) (w/w, SS: PAM).

4.4.3.2 ^{1}H-NMR Characterization

The chemical shifts of SS-PAM in different ratios of PAM derivative **b** showed in Table 4.6. All of these ratios of SS and PAM showed the chemical shift of proton in serine and tyrosine that shift to downfield. This downfield shift showed the change in the molecular environment that caused by chemical reaction. This shift was the result of the shielding effects of the triazine ring on the tyrosine residue. The same results of previous study (Cho, 2003) also reported that the proton peaks at 6.68 and 6.96 ppm of the tyrosine residue in sericin shifted downfield to 7.09 and 7.26 ppm, respectively. Because of the electron-

withdrawing effects of the carbonyl groups on ester linkage, the valence electron density around the protons connected to the carbon decreased (see Fig. 4.17). These results confirmed that the serine and tyrosine residues of the sericin reacted with PAM derivative.

Table 4.6 ^{1}H-NMR chemical shifts of modified sericin by chemical reaction (SS-PAM)

SS-PAM	Chemical shift (ppm)	Type of proton
1:1	3.746	Ser β
	4.120	Ser α
	7.049	Tyr ϕ (broad singlet peak)
1:5	3.818	Ser β
	4.149	Ser α
	7.055	Tyr ϕ (broad singlet peak)
1:10	3.869	Ser β
	4.123	Ser α
	7.055	Tyr ϕ (broad singlet peak)

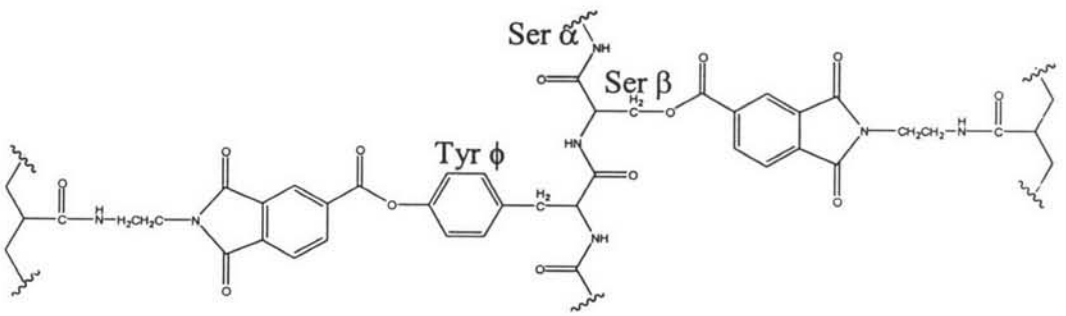

PAM derivative **b** sericin PAM derivative **b**

Figure 4.17 Chemical structure of modified sericin (SS-PAM).

4.4.3.3 Thermal Gravimetry Characterization

From TG/DTA curves of SS-PAM (1:1 wt/wt) (Fig. 4.18), the degradation temperature at 292°C was due to the loss of sericin in modified product. The weight loss of imide group remained 11.6% but the weight loss of sericin and %char were found up to 41.2 and 26.2%, respectively. These results suggested that the hydroxyl groups of sericin could react with carboxylic group and form some part of crosslink structure that was lost in higher temperature.

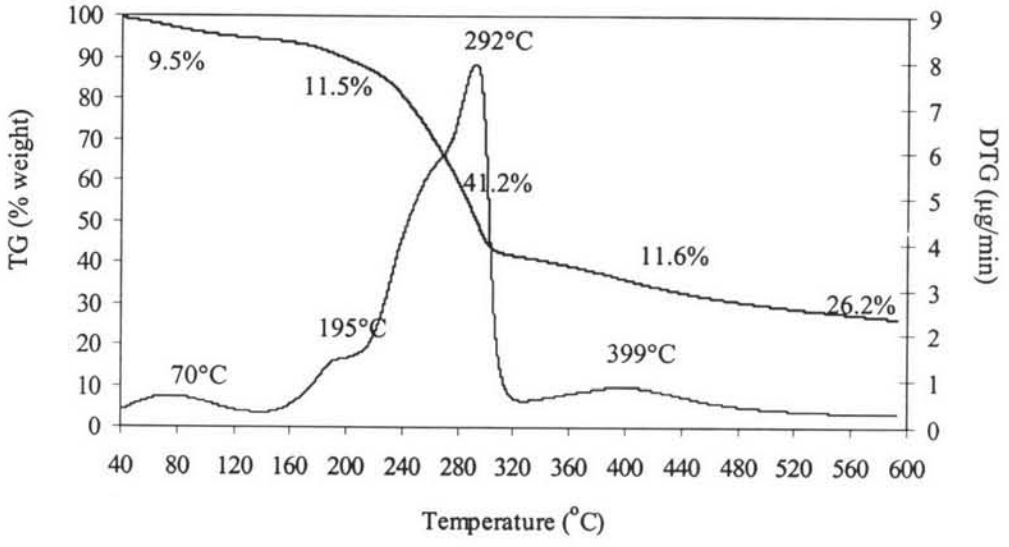

Figure 4.18 TG/DTA curves of SS-PAM (1:1 w/w).

From TGA results of SS-PAM modification in different ratios were shown in Table 4.7. The weight loss of sericin in these products was relative to the amount of sericin raw material and degradation temperature was observed about 293°C. Moreover, the weight loss of imide groups in these products was relative to the amount of PAM derivative **b** and degradation temperature was observed at 399°C.

Table 4.7 Temperature degradation and % weight loss of modified sericin by chemical reaction (SS-PAM)

SS-PAM (w/w)	Step of weight loss								% Char
	Water&EtOH		DMF&TMA		Decompositon of sericin		Decompositon of imide rings		
	Td_1 (°C)	%wt loss	Td_2 (°C)	%wt loss	Td_3 (°C)	%wt loss	Td_4 (°C)	%wt loss	
1:1	70	9.5	195	11.5	292	41.2	399	11.6	26.2
1:5	<100	8.1	214	11.0	288	30.8	399	17.3	32.8
1:10	<100	7.6	216	11.8	293	30.6	399	18.4	31.6

4.4.3.4 Gel Permeation Chromatography Characterization

Table 4.8 Retention time of sericin, PAM, modified sericin by chemical reaction (SS-PAM)

Sample	Retention time (min)
Sericin	16.533
PAM	21.621
SS-PAM (1:1)	23.808
SS-PAM (1:5)	25.655
SS-PAM (1:10)	26.182

Figure A23 showed the solubility of modified sericin by chemical reaction. Increasing the amount of PAM derivative content led to reducing the solubility in water of SS-PAM. This result confirmed that the hydroxyl groups of sericin were more substituted by PAM derivative and connected along chains to form crosslink (see Fig. 4.19). In GPC results showed the retention time of sericin, PAM,

and SS-PAM in Table 4.8. Increasing the amount of PAM derivative led to increasing the retention time that mean decreasing the molecular weight of dissolved SS-PAM. One reason could be due to the lower solubility of product due to higher degree of crosslinking in water that affected to GPC results

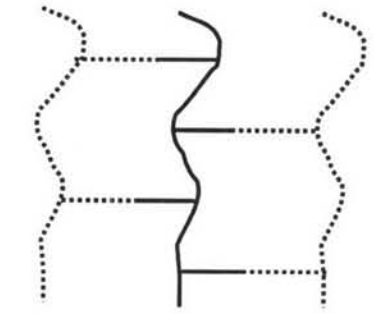

Figure 4.19 Crosslink structure between sericin and PAM derivative.

4.5 Electrospinning of Modified Sericin (SS-PAM)

4.5.1 Scanning Electron Microscope Characterization

SEM images (Fig. 4.20-4.22) showed the morphology of as-spun modified sericin by chemical reaction (SS-PAM) in 50% formic acid. For ratio of 1:1 w/w of SS-PAM were observed in Fig. 4.20. The morphology of the electrospun looked like flake and form dried film with high shrinkage so that cracking on surface was observed, especially when increased applied high voltage.

For ratio of 1:5 w/w of SS-PAM were observed in Fig. 4.21. The morphology of the electrospun product was spherical shape and the average size was observed as 2.44 μm and 3.16 μm for 40% and 50% (w/v), respectively. Fig. 4.22 exhibited nanoparticles of SS-PAM modification (1:10 w/w). The morphology of these particles was like a conical shape that was induced by stretching of tiny droplets. From image analysis with magnification 5000, the average size was measured as 202 and 238 nm for 40% and 50% (w/v) of concentration, respectively.

These results concluded that the average size was increased by increasing the concentration.

The applied voltage was varied between 15 and 25 kV for the ratios of 1:1, 1:5, and 1:10. All of these applied voltages were fixed for concentration of 50% (w/v) and collection distance at 15 cm. The SEM images of SS-PAM modification (1:5 w/w) at the concentration of 50% (w/v) were exhibited in Fig. 4.21 (a)-(b). The average size was measured as 2.61, 3.06, and 3.16 μm for applied voltage 15, 20 and 25 kV, respectively. The SEM images of SS-PAM modification (1:10 wt/wt) at the concentration of 50% (w/v) were exhibited in Fig. 4.22 (a)-(b). The average size was measured as 185, 202 and 239 nm for applied voltage 15, 20 and 25 kV, respectively. These results concluded that the average size was increased by increasing the applied high voltage.

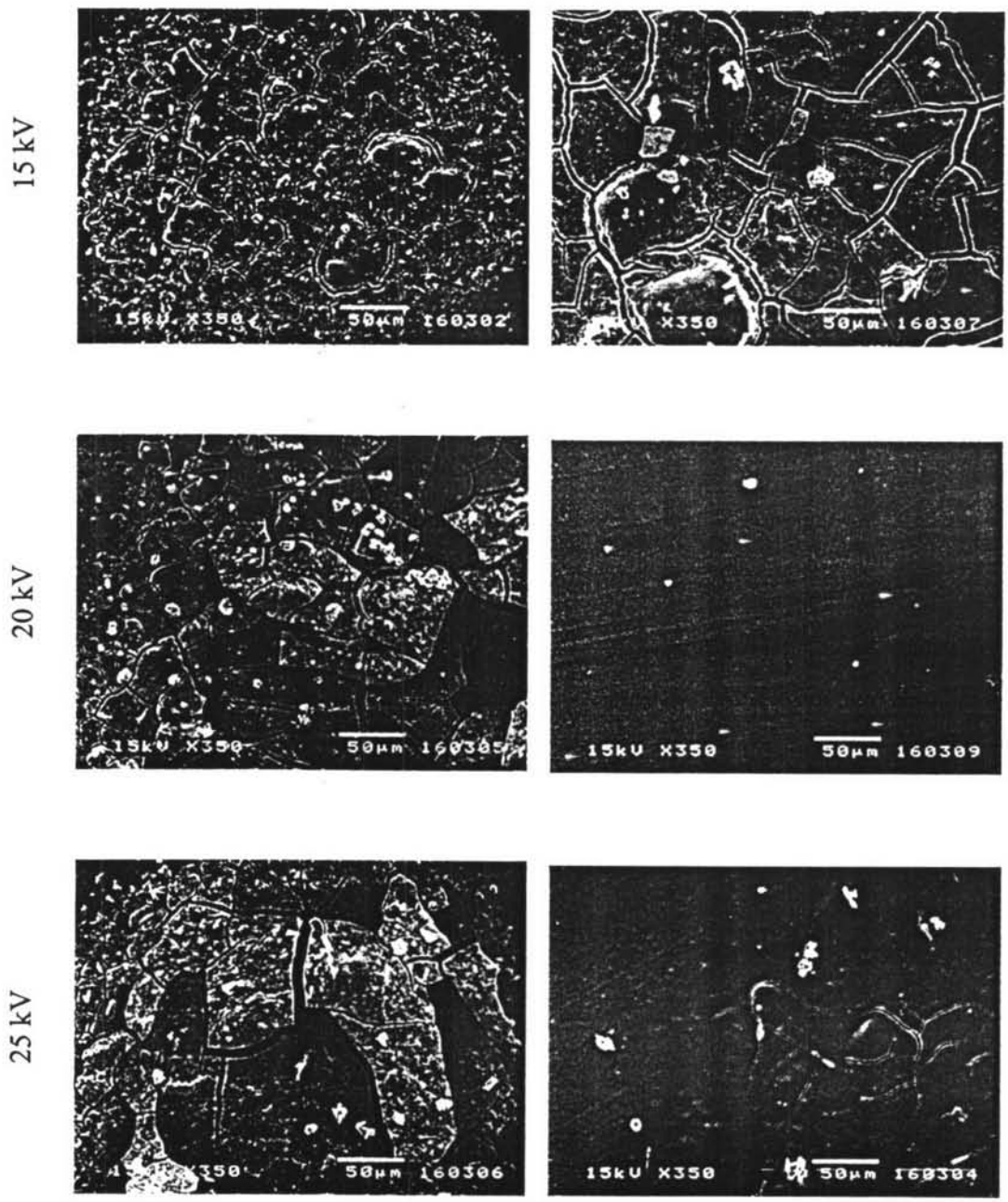

Figure 4.20 SEM images (at magnification of 350 and scale bar shown is for 50 µm) of electrospun modified sericin (SS-PAM) 1:1 w/w from: (a) 20% w/v; (b) 30% w/v in 50% formic acid.

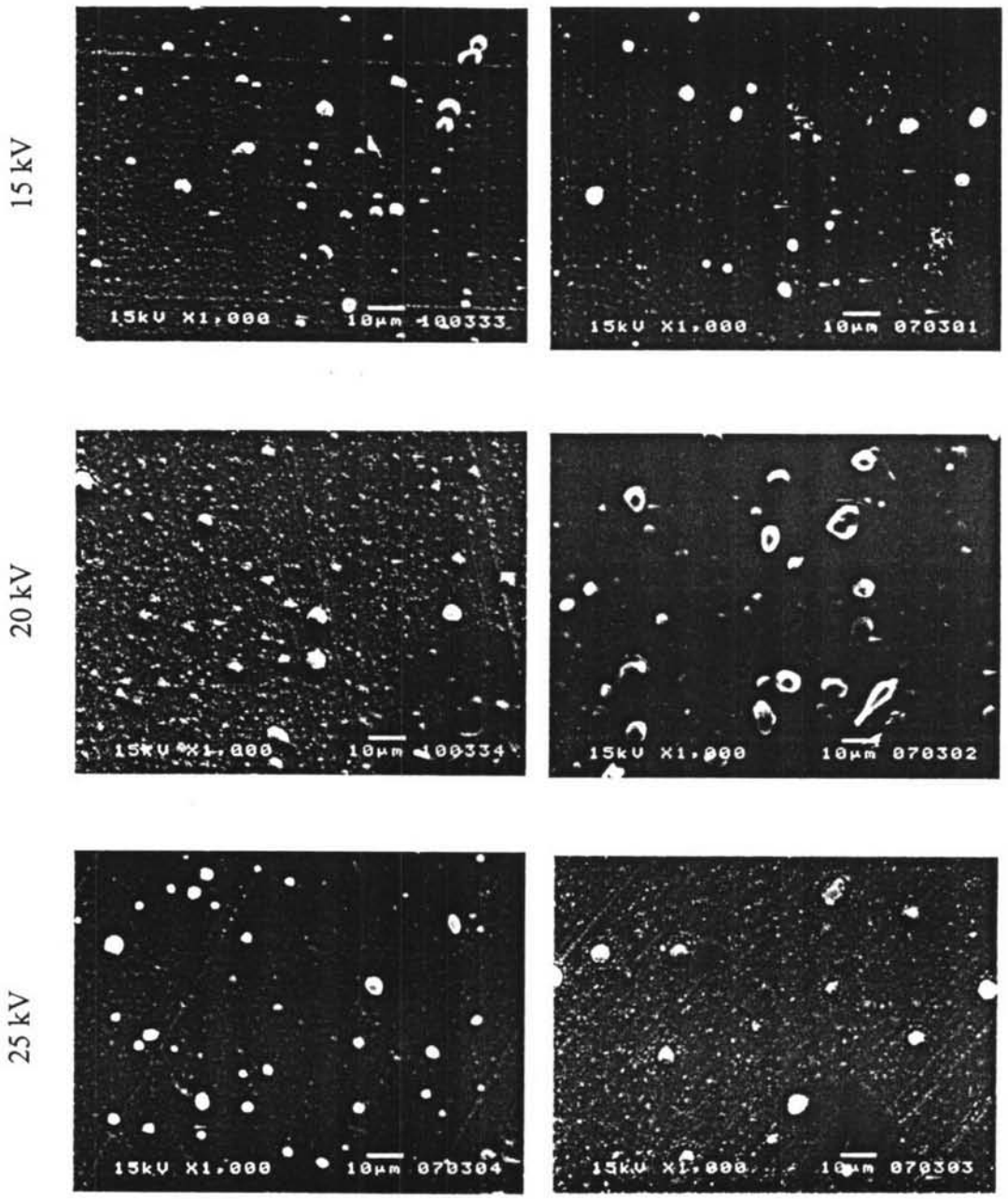

Figure 4.21 SEM images (at magnification of 1000 and scale bar shown is for 10 µm) of electrospun modified sericin (SS-PAM) 1:5 w/w from: (a) 40% w/v; (b) 50% w/v in 50% formic acid.

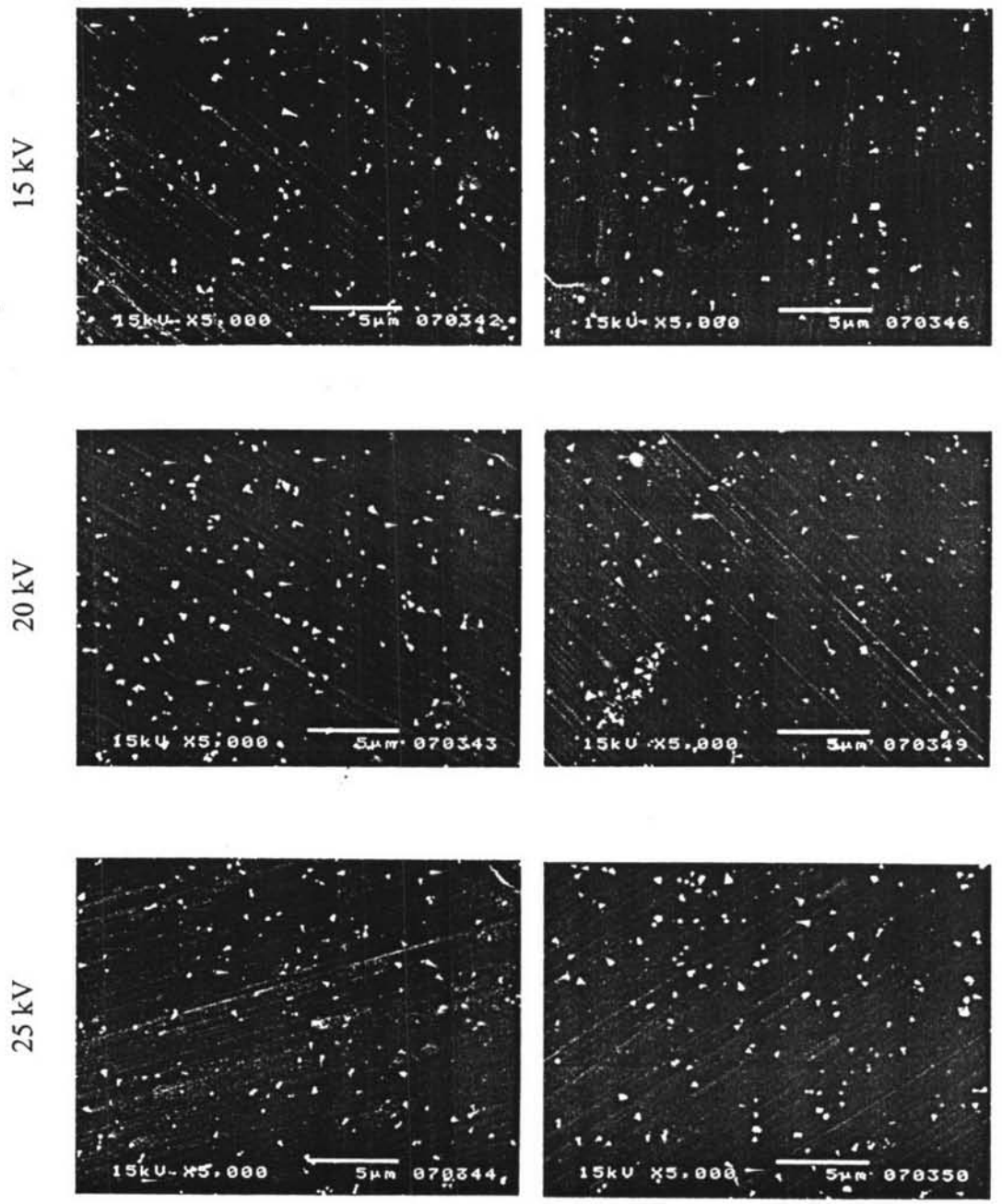

Figure 4.22 SEM images (at magnification of 5000 and scale bar shown is for 10 µm) of electrospun modified sericin (SS-PAM) 1:10 w/w from: (a) 40% w/v; (b) 50% w/v in 50% formic acid.